

Multi-speed Multi-load Bearing Diagnostics Using Extended Phase Space Topology

T. Haj Mohamad^{1,*}, C. A. Kitio Kwuimy^{2,**}, and C. Nataraj^{1,***}

¹Villanova Center for Analytics of Dynamic Systems (VCADS), Villanova University, Villanova, PA 19085, USA

²Department of Engineering Education, College of Engineering and Applied Science, University of Cincinnati, Cincinnati, OH 45221, USA

Abstract. This paper presents the application of Extended Phase Space Topology (EPST) and conventional statistical time domain features in the diagnostics of various bearing faults in rotating machinery systems. Bearings with various health statuses operating under multiple motor loads and speeds are analyzed. The results indicate remarkable performance in detecting anomalous behavior and in identifying faults with virtually perfect accuracy, recall and precision.

1 Introduction

There is considerable interest in rolling element bearing diagnostics due to their wide use in machines, and their failure is one of the most common reasons for machines breaking down. Predicting the potential breakdown of a machine can prevent catastrophic failures and production loss. Accurate prediction can also improve safety and reduce repair costs in most industries.

To this end, rolling element bearings are traditionally diagnosed using envelope analysis techniques [1–3]. Although these techniques are capable of extracting detailed information from the response of the system, they rely on expert knowledge and have to be carefully designed and adapted to a specific problem. For many applications, such as online/automated diagnostics, it is desirable to develop robust algorithms that can provide accurate results in order to identify faults and their severity quickly and in an automated fashion.

Our previous work [4–6] introduced and developed a family of methods based on the phase space characterization for different dynamical systems. In the present paper, we apply a novel feature extraction technique that we call Extended Phase Space Topology (EPST) [7–9] in order to detect and identify bearings with different health statuses under multiple motor operating conditions of load and speed.

The rest of this paper is organized as follows: In section 2, the experimental setup and measurement of data are introduced. Section 3 describes the mathematical details of the proposed feature extraction method. Section 4 discusses the results of fault identification. Finally, section 5 summarizes and concludes this paper.

*e-mail: thajmoha@villanova.edu

**e-mail: kwuimyck@ucmail.uc.edu

***e-mail: c.nataraj@villanova.edu

2 Experimental Setup

The proposed approach in this study was implemented on data collected from motor bearings provided by Case Western Reserve University [10, 11]. The experimental setup that was used in the study is shown in Fig. 1. The bearing experimental setup (shown in Fig. 1) consists of a 2-horsepower (hp) motor with a torque transducer/encoder and a dynamometer. The dynamometer was used to apply various loads on the motor. For this study, four motor loads of 0 to 3 hp (motor speeds of 1797 to 1720 RPM) were considered. Moreover, SKF deep groove ball bearings were used for the drive end (DE) and fan end (FE) bearings. Multiple test DE bearings were used with different health conditions including one healthy bearing (H) and three defective bearings with a ball defect (B), an inner race defect (IR) and an outer race defect (OR). Table 1 summarizes the collected data under various operating conditions.

Bearings with defective ball and inner race were seeded with single point faults with diameters of 0.007, 0.014 and 0.021 inches while bearings with outer race defect were seeded with faults of 0.007 and 0.014 diameter. For outer race defective bearings, the faults were seeded at a 6 o'clock position. The vibrational signals were recorded using accelerometers installed on the drive end and fan end bearing housing at a 12 o'clock position. The signal was recorded for approximately 20 seconds and 10 seconds for healthy and defective bearing conditions, respectively, at a sampling rate of 12,000 Hz.

3 Methodology

An overview of the fault detection procedure used in this paper is summarized in Fig. 2 and the procedure is described as follows. First, acceleration data of the drive end and fan end bearings were collected for various bearing

Table 1. Bearing data description of various conditions, fault diameters, motor loads and speeds.

| Bearing Condition | Fault Diameter | Motor Load | Motor Speed |
|------------------------------|----------------|------------|-------------|
| Healthy | 0 | 0 | 1797 |
| | | 1 | 1772 |
| | | 2 | 1750 |
| | | 3 | 1730 |
| Ball/ Inner race/ Outer race | 0.007/ 0.014 | 0 | 1797 |
| | | 1 | 1772 |
| | | 2 | 1750 |
| | | 3 | 1730 |
| Ball/ Inner race | 0.021 | 0 | 1797 |
| | | 1 | 1772 |
| | | 2 | 1750 |
| | | 3 | 1730 |

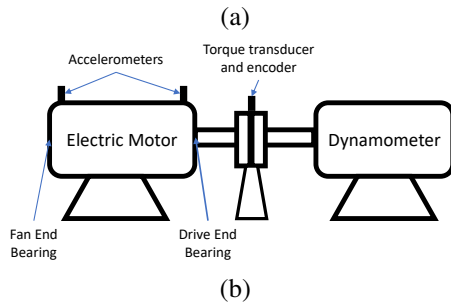
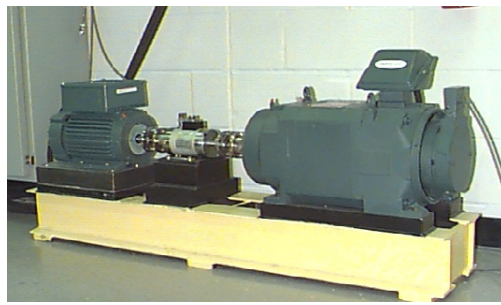


Figure 1. (a): The bearing experimental test [10]. (b): Schematic diagram of the test rig.

conditions, motor loads and shaft rotational speeds. The vibration data was then divided into multiple segments of one-second periods. For each segment, two sets of features were extracted using EPST and conventional statistical time domain features. The EPST method is based on characterizing the topology of the density distribution of the vibration data. The density distribution of the vibration signal is approximated using Legendre polynomials. The coefficients of the orthogonal polynomials are then used as features. Our previous work [7–9] explains in detail the derivation and the implementation of the EPST method. A linear support vector machine (SVM) with optimal parameters was built in order identify the bearing condition i.e., H, B, IR and OR using features of the EPST method.

In order to extract the EPST features, let $X=(x_1, x_2, \dots, x_n)$ be an independent and identically distributed sample data drawn from a distribution with an unknown density function Ψ . The shape of this function can be estimated by

its kernel density estimator ($\hat{\Psi}$ indicates that it is an estimate, and h indicates that its value can depend on h).

$$\hat{\Psi}_h(x) = \frac{1}{nh} \sum_{i=1}^n \Gamma\left(\frac{x-x_i}{h}\right) \quad (1)$$

where, $h > 0$ is a smoothing parameter called the bandwidth, and $\Gamma(\cdot)$ is the kernel function which satisfies the following requirements.

$$\int_{-\infty}^{\infty} \Gamma(u) du = 1 \quad (2)$$

$$\Gamma(-u) = \Gamma(u) \quad \forall u \quad (3)$$

There is a range of kernel functions that can be used, including uniform, triangular, biweight, triweight, Epanechnikov, normal, etc. Due to its conventional and convenient mathematical properties, we use the standard normal density function in our approach, defined as the following:

$$\Gamma(u) = \frac{1}{\sqrt{2\pi}} e^{-\frac{1}{2}u^2} \quad (4)$$

Let x be a state of the system and $y_d = \hat{f}_h(x)$, its density computed using the kernel density estimator. y_d is then approximated with Legendre orthogonal polynomials. Legendre polynomials can be directly obtained from Rodrigues' formula which is given by:

$$\Phi_m(x) = \frac{1}{2^m m!} \frac{d^m}{dx^m} [(x^2 - 1)^m], \quad m = 0, 1, 2, \dots \quad (5)$$

It can also be obtained using Bonnet's recursion formula:

$$(m + 1)\Phi_{m+1}(x) = (2m + 1)x\Phi_m(x) - m\Phi_{m-1}(x) \quad (6)$$

where the first two terms are given by:

$$\Phi_0(x) = 1, \quad \Phi_1(x) = x \quad (7)$$

The coefficients of the Legendre polynomials are obtained by using the least squares method assuming the following linear regression model:

$$\Psi(x, \beta) = \sum_{j=1}^m \beta_j \Phi_j(x) \quad (8)$$

Letting

$$X_{ij} = \frac{\partial \Psi(x_i, \beta)}{\partial \beta_j} = \Phi_j(x_i), \quad (9)$$

the estimated coefficients are given by:

$$\hat{\beta} = (X^T X)^{-1} X^T y_d \quad (10)$$

The coefficients $\hat{\beta}$ constitute the features in our approach that can be used in classification or regression problems. The approximated density using Legendre Polynomials is then calculated using the following:

$$\Psi_a = X \hat{\beta} \quad (11)$$

Root mean square error (RMSE) and Pearson's correlation coefficient (PCC) were calculated to compute the quality of the fit using the following equations:

$$\text{RMSE} = \sqrt{\frac{1}{N} Z Z^T}, \quad \text{PCC} = \frac{\sigma_d^T \sigma_a}{\sqrt{(\sigma_d^T \sigma_d)(\sigma_a^T \sigma_a)}} \quad (12)$$

where, $Z = (y_d - \Psi_a)$ is the residual vector, N is the number of points in the density function, $\sigma_d = (y_d - E\{y_d\})$ and $\sigma_a = (\Psi_a - E\{\Psi_a\})$. $E\{\cdot\}$ is the expected value.

In addition to the EPST features, various statistical features were extracted from the vibration data including both simple and high order statistics. Eight statistical features were computed including (1) mean, (2) root mean square (RMS), (3) standard deviation (SD), (4) peak value (PV), (5) minimum value (MV), (6) crest factor (CF), (7) kurtosis value (KV), and (8) skewness value (SV).

4 Results and Discussion

The EPST method, which is based on characterizing the topology of the density distribution of the vibration data, is applied by mapping the data onto a density space for each condition and then approximating these densities using Legendre polynomials. After the density plots were estimated, the plots were then approximated using Legendre polynomials of order 30. The order of Legendre polynomials was selected based on the best fit between the actual and the approximate densities by calculating the root mean square error (RMSE) and Pearson's Correlation Coefficient (PCC).

The extracted features were used as input to a linear SVM classifier in order to classify various bearing conditions (H, B, IR and OR). For each set of data, 36 features were used in the feature set for training (10 EPST features and 8 statistical features for each acceleration signal). Various SVMs were trained using 60% of the data samples (276 cases) and a cross validation algorithm with five folds. 40% of the data samples (184 cases) were used for testing the classifier. The box constrained parameter was optimized by minimizing the k-fold cross validation loss in order to find the optimal linear SVM.

To describe the performance of the classifier for the fault detection application, various metric rates were calculated from the confusion matrix such as precision, recall and overall accuracy. For each class, precision measures the rate of correct predictions out of all predictions

that were made by the classifier. In other words, when the classifier predicts a class, precision indicates how often the prediction is correct. Recall measures the correctly predicted rate of the actual samples for a given class. If the classifier has high recall and low precision for a certain class, this means that the classifier is biased to that class. A high precision and low recall classifier for a given class indicates that the classifier is too conservative. The classifier is less likely to predict the given class, but when it does predict it, it is very likely to be correct. Ideally, a classifier with high recall and high precision is what we seek. Finally, the overall accuracy of the classifier is the rate of the correct prediction.

The results can be summarized as follows.

- The classifier model was able to identify a hyperplane in the feature space that can separate all training set samples with 100% overall accuracy as shown in Table 2.
- The classification of the test data presented by means of the confusion matrix in Table 3 indicate an overall accuracy of 100% for predicting different bearing conditions.
- The classifier was able to detect anomaly behavior in the system by distinguishing between healthy and defective bearing conditions.
- The classifier was able to predict all the cases with 100% accuracy, 100% recall and 100% precision for each bearing condition.
- The extracted features provide valuable information about the bearing defect regardless of the fault level and severity.
- No a priori knowledge of the system was included in the extracted features. This implies the EPST approach can be conveniently applied to diverse dynamical systems in an automated process with minimal need for adaptation or reliance on expert knowledge about the system.

5 Conclusion

The study demonstrates that the EPST method combined with statistical measures provide very accurate references about the status of the health of bearings by exploiting the dynamical response. An optimal SVM was achieved using the extracted features in order to predict different bearing conditions. Furthermore, results show that the innovative EPST procedure has outstanding performance in fault detection and identification with a virtually perfect classification accuracy. For future work, a comparison with other bearing diagnostics techniques is necessary. Also, a severity analysis is needed to predict the fault diameter and the defect level, and is being pursued.

References

- [1] R.B. Randall, J. Antoni, Mechanical systems and signal processing **25**, 485 (2011)
- [2] V. Patel, N. Tandon, R. Pandey, Measurement **45**, 960 (2012)

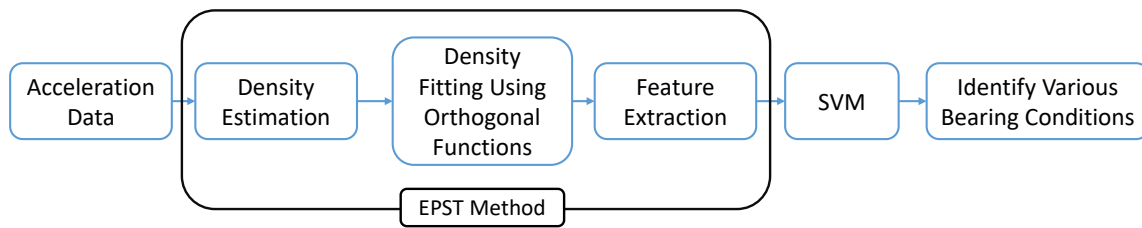


Figure 2. An overview of the bearing diagnostics method

Table 2. Prediction of various defect classes for training data.

| | | Training Confusion Matrix | | | | Recall | Precision |
|--------------|----|---------------------------|-------------|-------------|-------------|-----------------|-----------|
| Output Class | H | 84 30.4% | 0 0.0% | 0 0.0% | 0 0.0% | 100.0% | 100.0% |
| | B | 0 0.0% | 72 26.1% | 0 0.0% | 0 0.0% | 100.0% | 100.0% |
| | IR | 0 0.0% | 0 0.0% | 72 26.1% | 0 0.0% | 100.0% | 100.0% |
| | OR | 0 0.0% | 0 0.0% | 0 0.0% | 48 17.4% | 100.0% | 100.0% |
| | | H | B | IR | OR | Accuracy 100.0% | |
| | | Target Class | | | | | |

Table 3. Prediction of various defect classes for test data

| | | Test Confusion Matrix | | | | Recall | Precision |
|--------------|----|-----------------------|-------------|-------------|-------------|-----------------|-----------|
| Output Class | H | 56 30.4% | 0 0.0% | 0 0.0% | 0 0.0% | 100.0% | 100.0% |
| | B | 0 0.0% | 48 26.1% | 0 0.0% | 0 0.0% | 100.0% | 100.0% |
| | IR | 0 0.0% | 0 0.0% | 48 26.1% | 0 0.0% | 100.0% | 100.0% |
| | OR | 0 0.0% | 0 0.0% | 0 0.0% | 32 17.4% | 100.0% | 100.0% |
| | | H | B | IR | OR | Accuracy 100.0% | |
| | | Target Class | | | | | |

[3] Y. Ming, J. Chen, G. Dong, *Mechanical Systems and Signal Processing* **25**, 1773 (2011)

[4] M. Samadani, C.K. Kwuimy, C. Nataraj, *Diagnostics of a nonlinear pendulum using computational intelligence*, in *ASME 2013 Dynamic Systems and Control Conference* (American Society of Mechanical Engineers, 2013)

[5] M. Samadani, C.K. Kwuimy, C. Nataraj, *Communications in Nonlinear Science and Numerical Simulation* **20**, 583 (2015)

[6] T. Haj Mohamad, C. Nataraj, *Gear Fault Diagnostics Using Extended Phase Space Topology*, in *Annual Conference of the Prognostics and Health Management Society* (2017)

[7] T. Haj Mohamad, M. Samadani, C. Nataraj, *Journal of Vibration and Acoustics* (2018)

[8] M. Samadani, T. Haj Mohamad, C. Nataraj, *Feature Extraction for Bearing Diagnostics Based on*

the Characterization of Orbit Plots With Orthogonal Functions, in *ASME 2016 International Design Engineering Technical Conferences and Computers and Information in Engineering Conference* (American Society of Mechanical Engineers, 2016), pp. V008T10A026–V008T10A026

[9] T. Haj Mohamad, C.A.K. Kwuimy, C. Nataraj, *Discrimination of Multiple Faults in Bearings Using Density-Based Orthogonal Functions of the Time Response*, in *ASME 2017 International Design Engineering Technical Conferences and Computers and Information in Engineering Conference* (American Society of Mechanical Engineers, 2017), pp. V008T12A035–V008T12A035

[10] K. Loparo, <http://www.eecs.cwru.edu/laboratory/bearing/download.htm> (2003)

[11] W.A. Smith, R.B. Randall, *Mechanical Systems and Signal Processing* **64**, 100 (2015)